Title

AIPL1 implicated in the pathogenesis of two cases of autosomal recessive retinal degeneration.

Authors

Li, David
Jin, Chongfei
Jiao, Xiaodong
et al.

Publication Date

2014

Peer reviewed

Molecular Vision 2014; 20:1-14 <http://www.molvis.org/molvis/v20/1>
Received 9 December 2012 | Accepted 2 January 2014 | Published 6 January 2014

AIPL1 implicated in the pathogenesis of two cases of autosomal recessive retinal degeneration

David Li,[1] Chongfei Jin,[1,2] Xiaodong Jiao,[1] Lin Li,[1] Tahmina Bushra,[3] Muhammad Asif Naeem,[3] Nadeem H. Butt,[4] Tayyab Husnain,[3] Paul A. Sieving,[1] Sheikh Riazuddin,[3,4] S. Amer Riazuddin,[3,5] J. Fielding Hejtmancik[1]

(The first two and last two authors contributed equally to this manuscript.)

[1]Ophthalmic Genetics and Visual Function Branch, National Eye Institute, National Institutes of Health, Bethesda MD; [2]Eye Center of the 2nd Affiliated Hospital, Medical College of Zhejiang University, Hangzhou, China; [3]National Centre of Excellence in Molecular Biology, University of the Punjab, Lahore, Pakistan; [4]Allama Iqbal Medical College, University of Health Sciences, Lahore Pakistan; [5]The Wilmer Eye Institute, Johns Hopkins University School of Medicine, Baltimore MD

Purpose: To localize and identify the gene and mutations causing autosomal recessive retinal dystrophy in two consanguineous Pakistani families.

Methods: Consanguineous families from Pakistan were ascertained to be affected with autosomal recessive retinal degeneration. All affected individuals underwent thorough ophthalmologic examinations. Blood samples were collected, and genomic DNA was extracted using a salting out procedure. Genotyping was performed using microsatellite markers spaced at approximately 10 cM intervals. Two-point linkage analysis was performed with the lod score method. Direct DNA sequencing of amplified genomic DNA was performed for mutation screening of candidate genes.

Results: Genome-wide linkage scans yielded a lod score of 3.05 at θ=0 for D17S1832 and 3.82 at θ=0 for D17S938, localizing the disease gene to a 12.22 cM (6.64 Mb) region flanked by D17S1828 and D17S1852 for family 61032 and family 61227, which contains aryl hydrocarbon receptor interacting protein-like 1 (*AIPL1*), a gene previously implicated in recessive Leber congenital amaurosis and autosomal dominant cone-rod dystrophy. Sequencing of *AIPL1* showed a homozygous c.773G>C (p.Arg258Pro) sequence change in all affected individuals of family 61032 and a homozygous c.465G>T (p.(H93_Q155del)) change in all affected members of family 61227.

Conclusions: The results strongly suggest that the c.773G>C (p.R258P) and c.465G>T (p.(H93_Q155del)) mutations in *AIPL1* cause autosomal recessive retinal degeneration in these consanguineous Pakistani families.

Retinal dystrophies are debilitating disorders of the visual function that primarily affect the ocular retina. Among the inherited retinal dystrophies, retinitis pigmentosa (RP: OMIM 268000) contributes significantly to the total number of cases of blindness worldwide. RP, first described by the German physician Donders in 1857, refers to retinal degeneration with bone spicule-like pigmentation in the midperipheral fundus simulating inflammation [1]. The presenting visual symptom is usually night blindness, followed by loss of peripheral visual fields and progressing to loss of central vision, often ending in complete blindness [2]. RP primarily affects the rod photoreceptors with cone receptors becoming compromised only as the disease progresses [3]. Ocular findings comprise atrophic changes of the photoreceptors and the retinal pigment epithelium (RPE), followed by the appearance of melanin-containing structures in the retinal vascular layer [3]. The fundus appearance typically includes attenuated arterioles, bone spicule-like pigmentation, and waxy pallor of the optic disc. Affected individuals often have decreased or non-detectable rod responses in electroretinographic (ERG) recordings in the early stage of the disease, progressing to absent responses as the cones become compromised [3].

RP affects about 1 in 5,000 individuals worldwide, making it the most common inherited retinal dystrophy [4,5]. RP is genetically heterogeneous and can be inherited in an autosomal dominant, autosomal recessive, or X-linked recessive fashion. Autosomal dominant RP (adRP) comprises 15%–20% of all cases, autosomal recessive RP (arRP) comprises 20%–25% of cases, and X-linked recessive RP comprises 10%–15%. The remaining 40%–55% of cases, in which family history is absent, are called simplex (SRP), but many of these may represent autosomal recessive RP [6-10]. A large number of loci or genes have been associated with RP, including 36 for autosomal recessive RP in which the gene has been identified to date (RetNet).

Here we report two multiple-generation consanguineous Pakistani families with seven and six members affected by autosomal recessive retinal degeneration, respectively. Genome-wide scans localized the disease gene to

Correspondence to: J. Fielding Hejtmancik, MOGS/OGVFB/NEI/NIH, 5635 Fisher's Lane, Room 1127, Rockville, MD, 20852; Phone: (301) 496-8300; FAX: (301) 435-1598; email: f3h@helix.nih.gov

Table 1. Primers (5′-3′) used for sequencing of *AIPL1*

EXON1	AIPL1-E1-FW	TCCTCCTGGCTGGGTAAATC
	AIPL1-E1-RV	TTTTGGCACAGCTGAAAGC
EXON2	AIPL1-E2-FW	ATGGGGTGAACTGAGTGAGC
	AIPL1-E2-RV	GCTTGAGTCCCAGCTTTCC
EXON3	AIPL1-E3-FW	GCATAGTGAGGGAGCAGGAT
	AIPL1-E3-RV	TGGCTTATGAACCCTCTCGT
EXON4	AIPL1-E4-FW	AAGCATGACTTCAGGGAGATG
	AIPL1-E4-RV	GGGAGAAGGTCAGCCATGA
EXON5	AIPL1-E5-FW	TGCAGACCAAGGTCAGAGG
	AIPL1-E5-RV	GGTGGAGACAAGGTTTGGTG
EXON6	AIPL1-E6-FW	GGGATGGGGGATACAGAGAG
	AIPL1-E6-RV	CATGGGTGTGTCTGACTTTGA

chromosome 17p with two-point lod scores of 3.82 and 2.45 at θ=0, respectively. Fine mapping showed that the arRP locus cosegregates with markers in a 12.22 cM (6.64 Mb) interval containing the aryl hydrocarbon receptor interacting protein-like 1 (*AIPL1*) gene, in which affected individuals in family 61032 have a p.R258P and individuals in family 61227 a p.(H93_Q155del) homozygous missense mutation.

METHODS

Clinical ascertainment: Two hundred consanguineous Pakistani families with non-syndromic RP were recruited to participate in a collaborative study between the Center of Excellence in Molecular Biology, Lahore, Pakistan, and the National Eye Institute, Bethesda, MD, to identify genes causing congenital cataract and retinal degeneration when mutated. This study was approved by the Institutional Review Board (IRB) of the National Centre of Excellence in Molecular Biology and the CNS IRB at the National Institutes of Health. Participating subjects gave informed consent consistent with the tenets of the Declaration of Helsinki.

Family 61032 is from the Punjab province of Pakistan, and family 61227 is from the Sindh province. A detailed medical history was obtained by interviewing the patients and their family members. Ophthalmological examinations were performed either at the Rehmatullah Benevolent Trust (LRBT) Hospital or at the NCEMB, Lahore, Pakistan. The diagnosis of retinal degeneration was based on night blindness beginning in early childhood, progressive loss of peripheral vision, attenuation of retinal vessels and pigmentary retinopathy on fundus examination, and decreased or extinguished rod responses on electroretinogram. Electroretinogram responses were recorded using ERG equipment manufactured by LKC (Gaithersburg, MD) according to the standards of the International Society for Clinical Electrophysiology (ISCEV) [11]. Scotopic responses were recorded under dark adapted conditions using a single bright flash stimulus at 0 dB whereas the photopic responses were recorded under light adapted conditions using a 30 Hz flicker stimulus to a background illumination of 17–34 cd/m^2. Normal ranges calculated from 22 previous tracings of individuals of average age 41 years (14 years) using the same equipment under similar conditions in the Lahore facility are as follows: a wave: average amplitude=–196.9 (53.2) μV, latency=22.5 (1.6) ms; b wave amplitude=483.2 (81.3) μV, latency=44.8 (3.3) ms; flicker amplitude=107.5 (27.0) μV, latency=25.7 (2.5) ms. Comparable ERG tracings from control individuals of similar ages obtained under similar conditions at the same facility can be found [12-15]. Blood samples were collected from affected and unaffected family members. ACD anticoagulated venous blood samples were collected from affected and unaffected family members. DNA was extracted by a method described by Grimberg and colleagues [16].

Genotype analysis: Genome-wide linkage scans were performed with 382 highly polymorphic fluorescent markers from the ABI PRISM Linkage Mapping Set MD-10 (Applied Biosystems, Foster City, CA) with an average spacing of 10 cM. Based on the results of the initial genome-wide linkage scan, four markers (D17S1828, D17S1832, D17S1805, and D17S1791) were selected from the Marshfield map for fine mapping. Multiplex PCR were performed as previously described [17]. Briefly, each reaction was performed in a 5 μl mixture containing 40 ng genomic DNA, various combinations of 10 μM dye-labeled primer pairs, 0.5 μl 10X GeneAmp PCR Buffer II, 0.5 μl 10 mM dNTP mix, 2.5 mM $MgCl_2$, and 0.2 U of Taq DNA polymerase (Applied Biosystems). Amplification was performed in a GeneAmp PCR

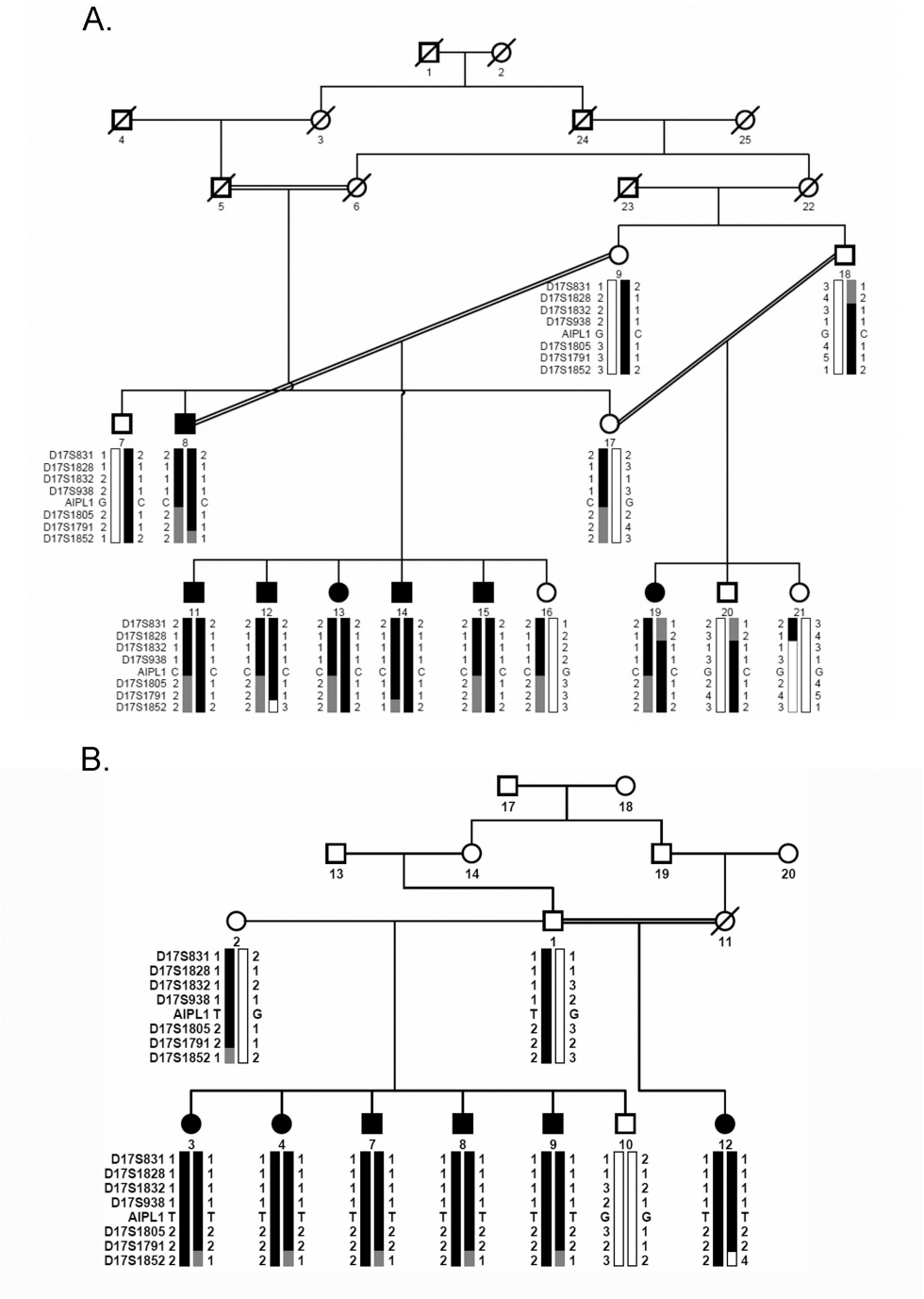

Figure 1. Pedigree drawing and chromosome 17p13 haplotypes of two familes. (**A**) family 61032 and (**B**) family 61227. Squares are males, circles are females, filled symbols are affected individuals, double line between individuals indicates consanguinity and diagonal line through a symbol is deceased family member. The haplotypes of 7 adjacent chromosome 17p13.2 microsatellite markers are shown. Alleles forming the risk haplotype are shaded black, alleles co-segregating with RP but not showing homozygosity are shaded grey, and alleles not co-segregating with RP are shown in white.

System 9700 (Applied Biosystems). Initial denaturation was performed for 5 min at 95 °C, followed by 10 cycles of 15 s at 94 °C, 15 s at 55 °C, and 30 s at 72 °C and then 35 cycles of 15 s at 89 °C, 15 s at 55 °C, and 30 s at 72 °C. The final extension was performed for 10 min at 72 °C and followed by a final hold at 4 °C. PCR products from each DNA sample were pooled and mixed with a loading cocktail containing HD-400 size standards (Applied Biosystems). The resulting PCR products were separated in an ABI 3130 DNA sequencer and analyzed by using GeneMapper 4.0 software package (Applied Biosystems).

Linkage analysis: Two-point linkage analysis was performed using the FASTLINK version of MLINK from the LINKAGE Program Package version 5.1 [18,19]. Maximum lod scores were calculated using ILINK. Autosomal recessive RP was

Table 2. Clinical characteristics of affected individuals in families 61032 and 61227

Family	ID	Gender	Age at Examination (yr)	Age at Onset (yr)	First Symptom	Visual Acuity	Nystagmus
61032	8	M	56	4	NB	NPL	yes
61032	11	M	16	3	NB	CF*	no
61032	12	M	22	4	NB	CF*	no
61032	13	F	19	3	NB	HM*	yes
61032	14	M	17	5	NB	CF*	no
61032	15	M	29	4	NB	HM*	yes
61032	19	F	21	3	NB	CF*	yes
61227	7	M	30	<4	NB	LP	yes
61227	8	M	28	<4	NB	LP	yes

*no peripheral vision; NB: night blindness; PL: light perception; NPL: no perception of light; CF: counting fingers; HM: hand motion

analyzed as a fully penetrant trait with an affected allele frequency of 0.001. The marker order and distances between markers were obtained from the Marshfield database and the National Center for Biotechnology Information (NCBI) chromosome 17 sequence maps. For the initial genome scan, equal allele frequencies were assumed; for fine mapping, allele frequencies were estimated from 100 unrelated and unaffected individuals from the Punjab province of Pakistan.

Mutation screening: Candidate genes were chosen from a 6.82 cM (4.7 Mb) interval on chromosome 17p flanked by markers D17S1828 and D17S1805. Primer pairs for individual exons were designed using the primer3 program. Individual exons of *AIPL1* were amplified with PCR using the primer pairs shown in Table 1. Amplifications were performed in 10 µl reactions containing 40 ng of genomic DNA, 8 picomoles of each primer, 2.5 mM of each dNTPs, 2.5 mM $MgCl_2$, and 0.2 U *Taq* DNA polymerase in the standard 1X PCR buffer provided by the manufacturer (Ampli*Taq* Gold Enzyme; Applied Biosystems). PCR amplification consisted of a denaturation step at 96 °C for 5 min, followed by 30 cycles, each consisting of 96 °C for 45 s followed by 57 °C for 45 s and at 72 °C for 1 min. PCR products were purified using the AMPure XP system (Beckman Coulter Biomek NX, Brea, CA). The PCR primers for each exon were used for bidirectional sequencing using the Big Dye Terminator Ready reaction mix according to the manufacturer's instructions (Applied Biosystems). Sequencing products were purified using the Agencourt CleanSEQ system (Beckman Coulter Biomek NX). Sequencing was performed on an ABI PRISM 3130 Automated sequencer (Applied Biosystems). Sequencing results were analyzed using Mutation Surveyor v3.30 (Soft Genetics, State College, PA) or Lasergene 8.0 (DNASTAR, Madison, WI).

Molecular modeling: The tetratricopeptide (TPR) repeat domains of wild-type and R258P AIPL1 were modeled using SWISS-MODEL. The 117 aa sequence extending from V180 to S296 was used in a BLAST search to identify the monomer template 3rkv.1.A solved at a resolution of 2.41 Å. The template shared 31% sequence identity with the AIPL1 TPR domain and had coverage of 99%. Analysis was performed in automatic mode using default parameters. The domain structure of AIPL1 was taken from NCBI and UniProtKB/Swiss-Prot (Q9NZN9.2).

Splice site prediction: Splice site prediction was performed with the Berkeley Drosophila Genome Project Neural Network splice site prediction algorithm [20] and the Technical University of Denmark Center for Biologic Sequence Analysis NetGen2 Server [21] using default settings. The Berkeley Drosophila Genome Project Neural Network splice site prediction algorithm identified neither the wild-type nor the mutant intron 3 5′ (donor) splice site, suggesting that even the wild-type might be a weak splice site. However, the Technical University of Denmark Center for Biologic Sequence Analysis NetGen2 Server implementation identified the wild-type splice site with a confidence level of 0.88. Using this algorithm, a score of 95% predicts splice sites that with high confidence, while nearly all true donor sites yield scores of 50% or greater. No other potential donor splice sites were identified in the surrounding 400 bp.

RESULTS

The pedigree in family 61032 showed an autosomal recessive inheritance pattern with a pseudodominant effect in the offspring of affected individuals 8 and 9, while the pedigree of family 61227 showed a straightforward autosomal recessive inheritance pattern in which one affected individual was the product of a first-cousin mating (Figure 1). Affected

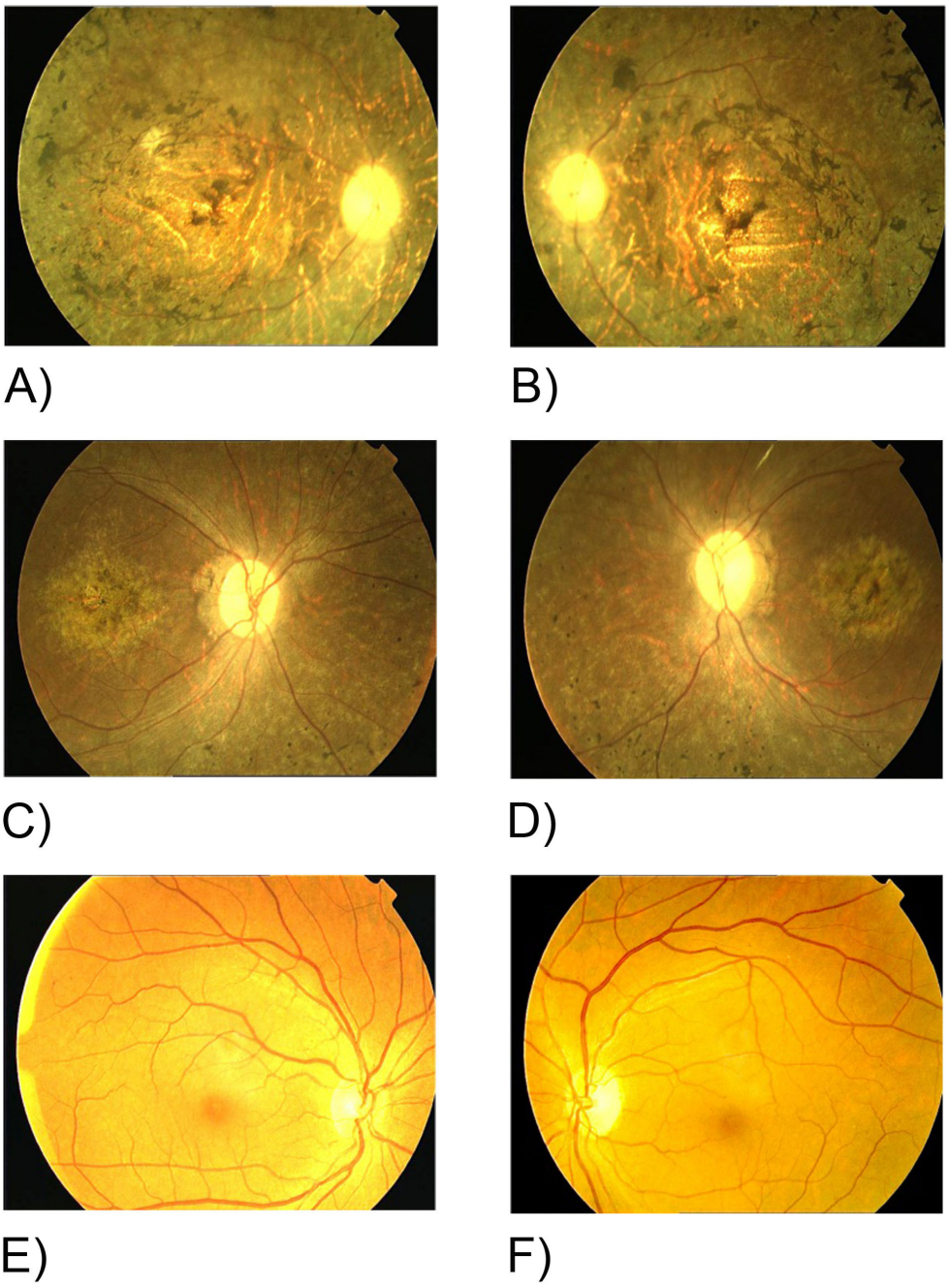

Figure 2. Fundus photographs of family of members of family 61032. **A**–**B**: Oculus dexter (OD) and oculus sinister (OS) of an affected 58-year-old individual (08). **C**–**D**: OD and OS of an affected 21-year-old individual (19). **E**–**F**: OD and OS of an unaffected 19-year-old individual (20). Fundus photographs of both affected individuals show bone spicule-like pigmentation that is more prominent in the midperiphery, pale waxy disc, and attenuated arterioles. The fundus photographs of the unaffected individual show no signs of retinitis pigmentosa (RP).

individuals from both families have no recollection of having vision or carrying out common early visual activities. All affected individuals in family 61032 were diagnosed with RP in the early years of their lives, experiencing night blindness beginning at 3–5 years of age, suggesting the onset of retinal degeneration at or before that time. Vision of all affected individuals at the time of examination was limited to light perception or hand motion with no peripheral vision. Individuals 8, 13, 15, and 19 showed nystagmus while individuals 11, 12, and 14 did not. Affected individuals in family 61227 also showed signs of retinal degeneration early in life. They were not examined until approximately 25–30 years of age, but at that time showed only light perception. Both had horizontal nystagmus (Table 2). According to the patients' medical records and history, the disease in all affected individuals progressed from night blindness with gradual decreasing visual acuity and progressive loss of peripheral vision. Fundus photographs were available only for members

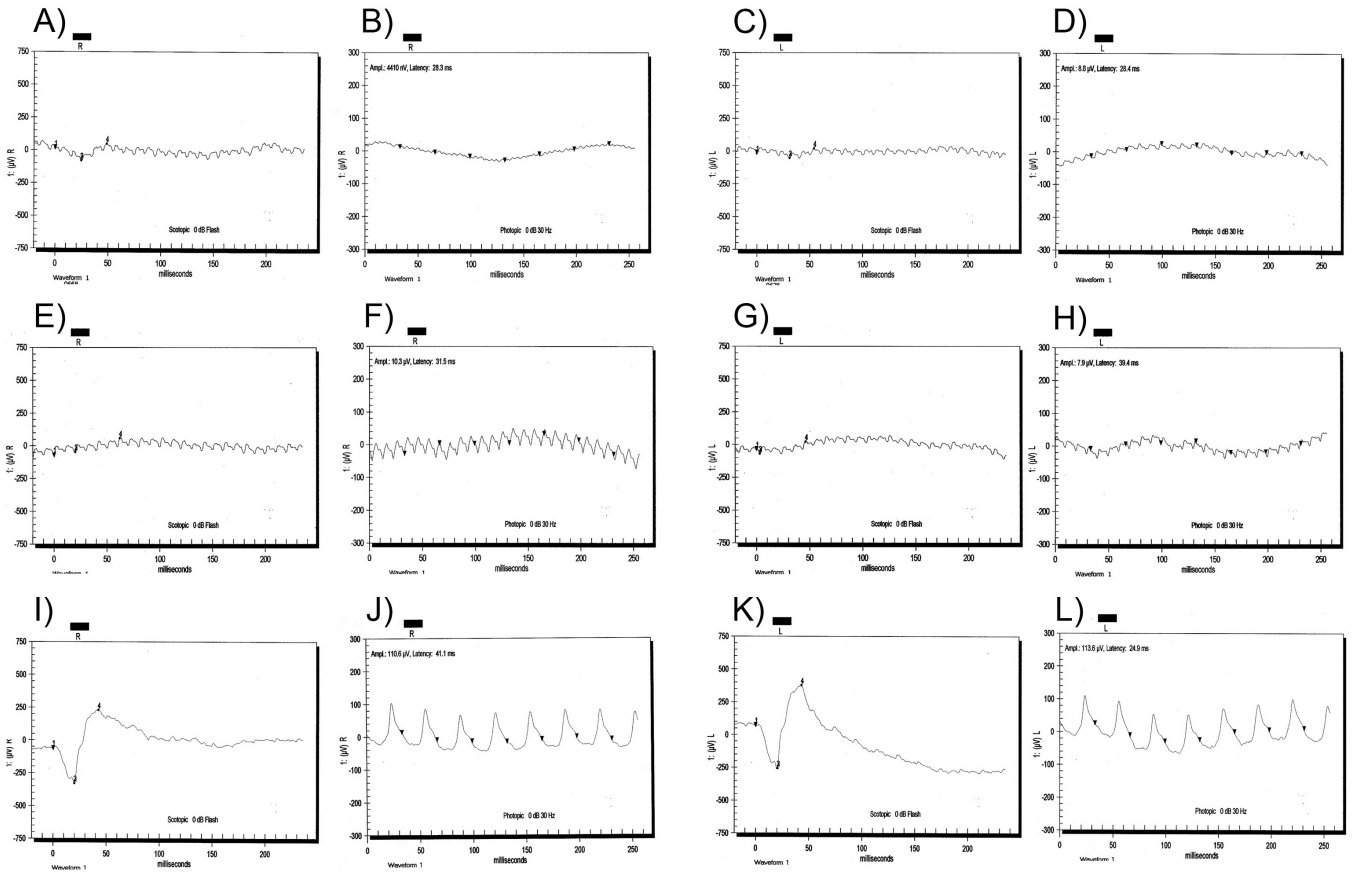

Figure 3. Electroretinography responses of members of 61032. Electroretinogram recordings of individual 08 (affected, 56 years old): **A**: Oculus dexter (OD) combined rod and cone response, **B**: OD cone response, **C**: Oculus sinister (OS) combined rod and cone response, and **D**: OS cone response; individual 19 (affected, 21 years old): E) OD combined rod and cone response, **F**: OD cone response, **G**: OS combined rod and cone response, and **H**: OS cone response; and individual 20 (unaffected, 19 years old): **I**: OD combined rod and cone response, **J**: OD cone response, **K**: OS combined rod and cone response, **L**: OS cone response.

of family 61032. Affected individuals showed typical signs of RP, including waxy pale optic discs, attenuation of retinal arteries, and bone spicule-like pigment deposits in the midperiphery of the retina (Figure 2A-D). No attenuation of retinal arteries and bone spicule-like pigment deposits were detected in the fundus photographs of the unaffected individuals in the family (Figure 2E–F). ERG recordings, also available only for individuals in family 61032, documented extensive loss of rod and cone function typical of advanced arRP in affected members as shown in Figure 3A-H, whereas the unaffected family members including carriers were within normal ranges with all amplitudes above average and latencies below average, thus showing no changes characteristic of RP (Figure 3I-L). Taken together, the ophthalmological examinations in both families showed typical features of retinal dystrophies and fulfilled the diagnostic criteria of RP. However, given the uncertainty in the age of onset, we cannot conclusively differentiate between Leber congenital amaurosis (LCA) and autosomal recessive RP.

Initially, all previously reported retinitis pigmentosa loci were excluded for linkage with a lod < −2 using primer pairs for markers specific for known loci. Linkage scans in both families localized the disease region to chromosome 17 (Table 3). During a genome-wide scan for family 61032, a lod score greater than 2.0 was obtained only for marker D17S938 with a lod=3.82 at θ=0 in family 61032 (Figure 4). Only seven additional markers gave lod scores greater than 0, D1S2797, D2S160, D4S1539, D6S287, D10S547, D13S285, and D18S478, each of which yielded a lod=1.2. In contrast to the chromosome 17 locus (see the following paragraph and Figure 1), examination of these regions indicated that the positive lod scores resulted from uninformative individuals who underwent obligate recombination events with nearby markers. In addition, among the markers selected for fine mapping of the chromosome 17 locus, D17S1832 yielded a lod score of 3.05

Table 3. Two point lod scores of markers on chromosome 17p13.2.

Family 61032			**θ**								
Marker	cM	Mb	0	0.01	0.05	0.1	0.2	0.3	0.4	*Zmax*	*θmax*
D17S831*	6.6	1.91	-2.58	-0.09	0.48	0.61	0.56	0.35	0.09	0.61	0.1
D17S1828	10.02	3.81	-1.56	0.52	1.22	1.35	1.19	0.84	0.42	1.35	0.1
D17S1832	13.07	5.97	3.05	3.04	2.93	2.71	2.11	1.42	0.69	3.05	0
D17S938*	14.69	6.18	3.82	3.74	3.39	2.95	2.02	1.07	0.24	3.82	0
AIPL1(c.773G>C)		6.32	4.26	4.18	3.82	3.37	2.43	1.48	0.6	4.26	0
D17S1805	16.84	8.51	-0.86	0.62	1.27	1.42	1.26	0.9	0.45	1.42	0.1
D17S1791	17.92	9.07	-0.46	1.2	1.85	1.94	1.64	1.12	0.53	1.94	0.1
D17S1852*	22.24	10.45	- ∞	-0.76	0.38	0.65	0.56	0.24	-0.03	0.65	0.1
Family 61227			**θ**								
Marker	cM	Mb	0	0.01	0.05	0.1	0.2	0.3	0.4	*Zmax*	*θmax*
D17S831*	6.6	1.91	2.00	1.96	1.78	1.56	1.10	0.65	0.23	2.00	0.00
D17S1828	10.02	3.81	0.67	0.65	0.58	0.48	0.30	0.16	0.06	0.67	0.00
D17S1832	13.07	5.97	3.66	3.59	3.31	2.96	2.21	1.41	0.59	3.66	0.00
D17S938*	14.69	6.18	2.45	2.41	2.21	1.96	1.46	0.94	0.43	2.45	0.00
AIPL1(c.465G>T)		6.32	4.04	3.97	3.68	3.31	2.52	1.66	0.78	4.04	0.00
D17S1805	16.84	8.51	3.66	3.59	3.31	2.96	2.21	1.41	0.59	3.66	0.00
D17S1791	17.92	9.07	2.00	1.96	1.78	1.56	1.10	0.65	0.23	2.00	0.00
D17S1852*	22.24	10.45	-0.09	1.54	2.00	1.98	1.61	1.04	0.38	2.02	0.07

* Marker included in genome wide scan

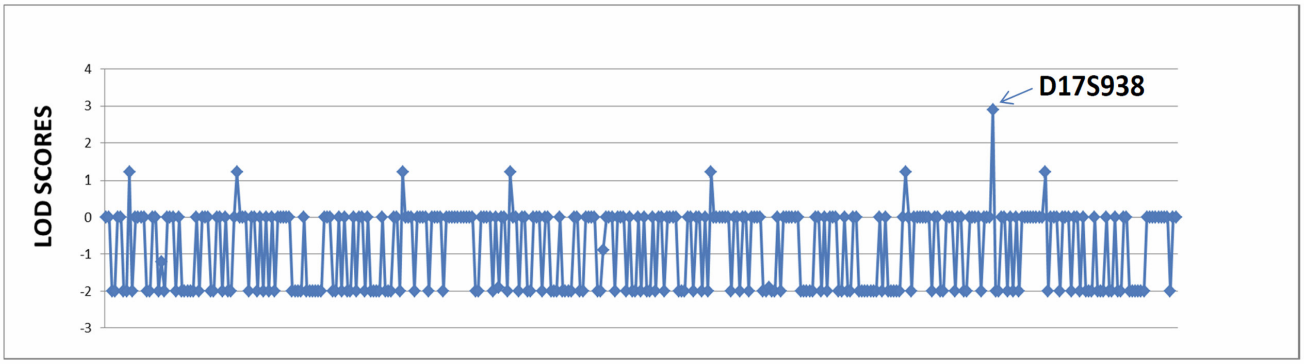

Figure 4. Graphical illustration of the two point lod scores obtained across 22 chromosomes during the genome-wide scan (note: lod scores less than -2 are considered exclusionary and shown as -2 for graphical purposes). We identified a single marker showing significant linkage with a lod score 0f 3.82 at θ =0 for D17S938.

at θ=0 (Table 3). Thus, two-point linkage mapping in family 61032 localized the causative gene to a 12.22 cM (6.64 Mb) region flanked by D17S1828 and D17S1852. Analysis of these markers in family 61227 showed maximum lod scores of 3.66 with D17S1832 and D17S1805. However, obligate recombination events were not present in this region, and occurred only with D17S1852, 16 cM (10 Mb) centromeric of AIPL1. Maximum lod scores of 4.26 and 4.04 were obtained with the

(A)

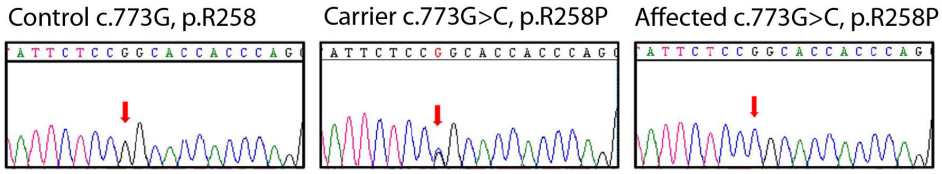

(B)

	H_{252}	T_{253}	S_{254}	D_{255}	I_{256}	L_{257}	R_{258}	H_{259}	H_{260}	P_{261}	G_{262}	I_{263}	V_{264}
Human	H	T	S	D	I	L	R	H	H	P	G	I	V
Chimp	H	T	S	D	I	L	R	H	H	P	G	I	V
Gorilla	H	T	S	D	I	L	R	H	H	P	G	I	V
Orangutan	H	T	S	D	I	L	R	H	H	P	G	I	V
Rhesus	H	T	S	D	I	L	R	H	H	P	G	I	V
Baboon	H	T	S	D	I	L	R	H	H	P	G	I	V
Tree shrew	H	T	S	D	I	L	R	Q	H	P	G	I	V
Mouse	H	T	S	D	I	L	R	H	H	P	G	I	V
Rat	H	T	S	D	I	L	R	H	H	P	G	I	V
Guinea pig	H	T	S	D	I	L	R	H	H	P	G	I	V
Rabbit	H	T	S	D	I	L	R	H	H	P	G	I	V
Dolphin	H	T	S	D	I	L	R	H	H	P	G	M	V
Cow	H	T	S	D	I	L	R	H	H	P	G	I	A
Horse	H	T	S	D	I	L	R	H	H	P	G	I	V
Dog	H	T	S	D	I	L	R	L	H	P	G	I	V
Megabat	H	T	S	D	I	L	R	Q	H	P	G	I	V
Hedgehog	H	T	S	D	I	L	R	H	H	P	G	I	G
Elephant	H	T	S	D	I	L	R	H	H	P	G	I	V
Opossum	H	S	S	D	I	L	R	H	H	P	G	I	A
Chicken	H	T	T	E	L	L	Q	K	H	N	D	N	A
Zebrafish	H	T	S	D	I	I	N	Q	H	P	G	G	T

Figure 5. Sequence chromatograms and alignment of *AIPL1* Arg 258 in 19 species. **A**: Electropherograms show the normal control sequence (left), carrier sequence (middle) and affected sequence (right) surrounding the *AIPL1* c.773G>C mutation. **B**: Amino acid sequence alignment around the *AIPL1* R258 residue (red) in 21 species ranging from human to zebrafish. R258 is part of a highly conserved region, suggesting that the R258P change would be highly deleterious for protein structure and enzymatic activity.

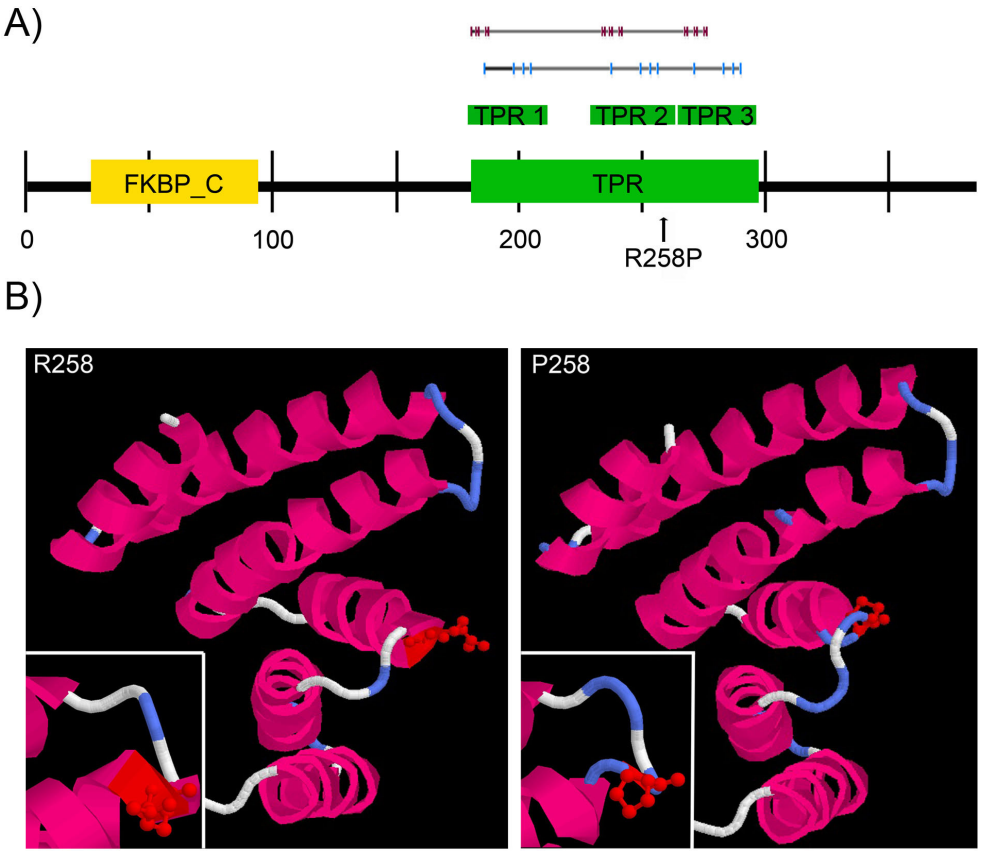

Figure 6. Sequence chromatograms and predicted effects of the splice site mutation. **A**: Sequence chromatograms of an unaffected individual, a heterozygote carrier, and an affected individual showing the c.465G>T mutation in relation to the exon and consensus splice site, with encoded amino acids shown above the DNA sequence. **B**: Exon structure of the *AIPL1* gene with the c.465G>T mutation shown at the end of exon 3 and the predicted skipping of exon 3 in the spliced mRNA. **C**: Protein and domain structure of the AIPL1 protein with the predicted in-frame p.(H93_Q155) deletion shown in red.

AIPL1 c.773G>C and c.465G>T mutations in families 61032 and 61277, respectively.

Visual inspection of the haplotypes supports the results of the linkage analysis in both families. In family 61032, there was a proximal recombination between individuals 18 and 8 at D17S1828 (Figure 1A). Similarly, there was a distal recombination between individuals 9 and 12 at D17S1852 (Figure 1A). This places the disease locus in a 12.22 cM (6.64 Mb) interval flanked by markers D17S1828 and D17S1852. Lack of homozygosity in affected individuals 8, 11, 12, 13, 15, and 19 at markers D17S1805 and D17S1791 further suggests that the pathogenic mutation lies proximal to marker D17S1805, in a 6.82 cM (4.7 Mb) interval flanked by markers D17S1828 and D17S1805. Alleles for D17S1832 and D17S938 are homozygous for all affected individuals. In family 61227, no telomeric recombination could be identified, but a centromeric recombination occurred between D17S1791 and D17S1852 in individuals 1 and 12 (Figure 1B). Although consanguinity in the mating between individuals 1 and 2 could not be verified by family history, homozygosity for nearby markers and the *AIPL1* mutation (see below) in all affected individuals strongly suggest a common origin for the causative mutation. Thus, lack of homozygosity for marker D17S1852 in affected individuals 3, 4, 7, 8, and 9 suggests the marker lies in a 12 cM (7 Mb) region flanked by D17S1828 and D17S1852.

There are three known candidate genes in the overlapping linked regions on chromosome 17p13.1, guanylate cyclase 2D (*GUCY2D*), *AIPL1,* and phosphatidylinositol transfer membrane-associated family member 3 (*PITPNM3*). The sequence changes identified in *GUCY2D* and *PITPNM3* in both families were either known single nucleotide polymorphisms or noncoding polymorphisms. Sequencing of all coding exons, exon-intron boundaries, and the 5′ untranslated region of these genes showed a single novel missense mutations in each family in *AIPL1* (Figure 5 and Figure 6). All affected individuals in family 61032 carry a homozygous G>C single base change at this position in exon 5 (c.773G>C, p.R258P). This sequence change was not seen in 100 ethnically matched controls or in the 1000 Genome or dbSNP databases. The amino acid sequence in the entire region surrounding the mutation is relatively well conserved, and R258 is conserved among all mammals, with conservative changes (Q and N) in the chicken and zebrafish, respectively (Figure 5). The c.773G>C, p.R258P change is estimated to be possibly damaging by PolyPhen-2, tolerated by SIFT, and neutral by CONDEL, which incorporates information from

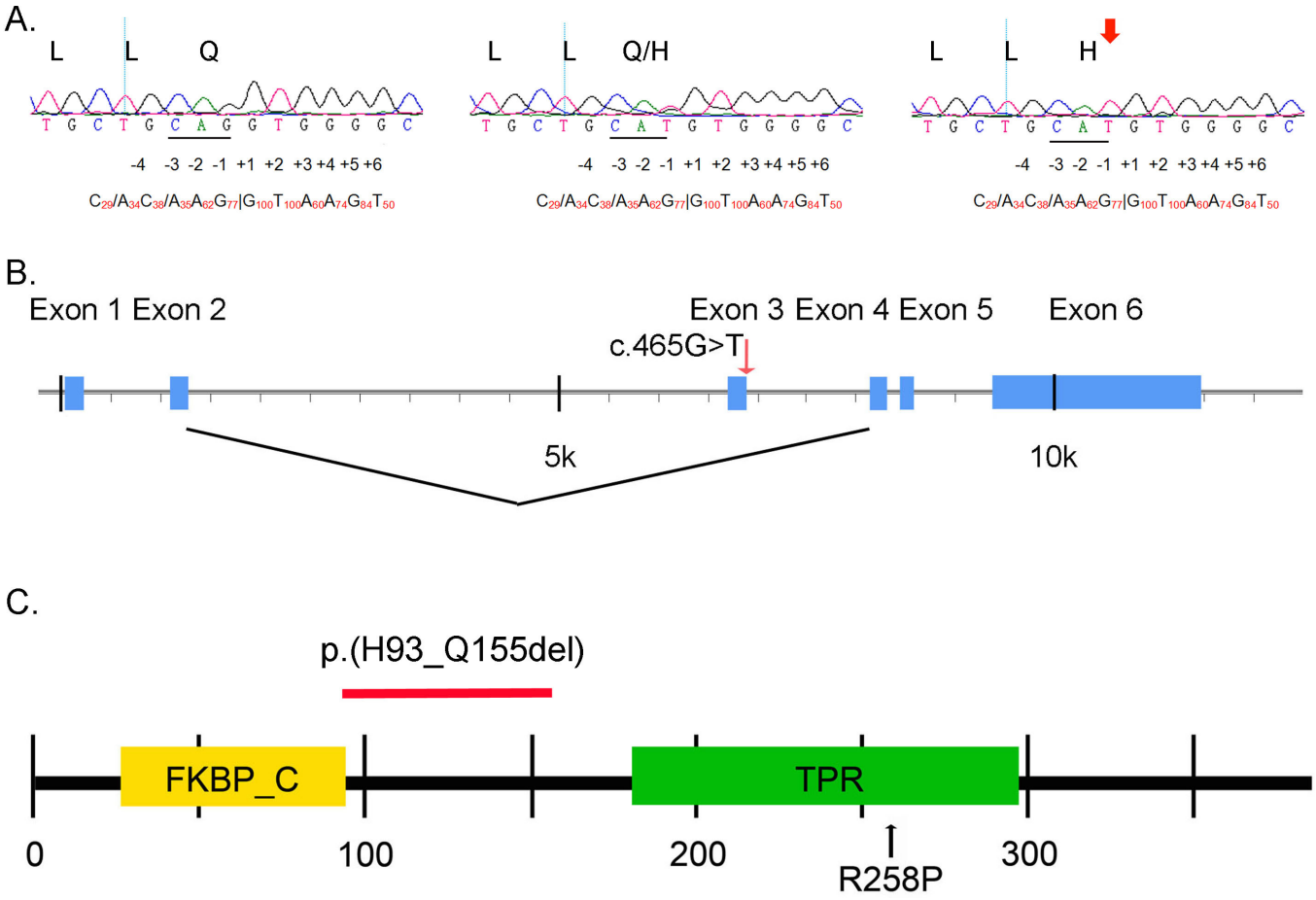

Figure 7. AIPL1 protein domains, structure, and the effect of the R258P mutation. **A**: *AIPL1* domains including the FKBP-type peptidyl-prolyl cis-trans isomerase (FKBP_C, yellow) domain, The tetratricopeptide repeat (TPR, green) domain, with three individual repeat domains (TPR1, TPR 2, and TPR 3, smaller green rectangles above the ruler), individual TPR motifs (blue tics above the TPR domain), and binding surfaces (maroon tics above the TPR domain). **B**: Modeled structures of theR258 (left) and P258 (right) 117 amino acid AIPL1 TPR domains with alpha helices shown in pink, turns shown in blue, and random coils shown in white. The R258 and P258 residues are shown in ball-and-stick form in red. The insets at the bottom left corner of each panel show the R258 residue residing near the end of the alpha helix of the second TPR repeat domain, and the P258 residue disrupting the helical structure so that the helix is shortened and the P258 and adjacent residues assume a turn structure.

the PolyPhen-2, SIFT, and MutationAssessor programs. However, this change lies within the second repeat unit of the TPR domain of the AIPL1 protein (Figure 7A). The R258P mutation is predicted by molecular modeling to disrupt the end of the second helix of the second TPR repeat domain, altering the secondary structure of this and the surrounding amino acid residues from an alpha helix to a turn structure, a significant change for the highly conserved TPR domain (Figure 7B).

Affected individuals in family 61227 are all homozygous for the c.465G>T sequence change. This sequence change was not seen in 100 ethnically matched control individuals nor does it occur in the 1,000 Genome or dbSNP databases. This nucleotide change alters a highly conserved Q155 amino acid to a histidine. This residue is conserved among mammals except the armadillo and shows only conservative changes through reptiles and fish, and is predicted to be damaging by SIFT [22], probably damaging by PolyPhen2 [23], and neutral by Condel [24]. However, the sequence change also alters the 5′ (donor) splice site for intron 3, reducing the score on the NetGen2 server from 0.88 to “not detectable”. No other likely donor splice sites were identified in the surrounding 400 bp; thus, this sequence change is predicted to result in in-frame skipping of exon 3 with a resulting p.(H93_Q155del) in-frame deletion in the AIPL1 protein.

DISCUSSION

Here, we report linkage of autosomal recessive retinal degeneration in two consanguineous Pakistani families to markers on chromosome 17p13.2. A genome-wide linkage scan in family 61032 excluded a large part of the genome and identified a single marker, D17S938, showing a lod score greater than 1.2. A maximum two-point lod score of 3.82 was obtained with D17S938 at θ=0, and the autosomal recessive RP locus cosegregates with chromosome 17p markers in a 12.22 cM (6.64 Mb) interval flanked by markers D17S1828 and D17S1852, and a lod score of 4.26 was obtained when analyzing the mutation as a linkage marker. This lies just above the 3 lod support limit, corresponding to a confidence limit of approximately 2×10^{-4}. Lack of homozygosity in affected individuals for markers D17S1805 and D17S1791 further suggests that the pathogenic mutation lies in a 6.82 cM (4.7 Mb) interval flanked by markers D17S1828 and D17S1805. The maximum lod score of 4.04 in family 61227 yields similar results, although the predicted severity of the sequence change in this family provides additional assurance that disease in this family results from the *AIPL1* mutation.

The presence of consanguinity in these families presents advantages and disadvantages for linkage analysis. Although consanguinity increases the power of linkage analysis dramatically, it is also increases the possibility that small homozygous regions will be shared between various members of the pedigree. If the region is small enough, it might be missed by the average 10 cM spacing of markers from the ABI MD-10 panels (Applied Biosystems) used in the genome-wide linkage screen. However, inheritance of the IBD mutation through a common founder in the previous four generations increases the probability of a fairly large linked region, and the use of two point rather than multipoint analysis decreases the chance of missing linked loci within 5–10 cM of a marker, even in the presence of a double recombination event.

Three known candidate genes, *GUCY2D*, *AIPL1*, and *PITPNM3*, reside in the critical interval. The former two genes have been associated with LCA (autosomal recessive) and autosomal dominant cone-rod dystrophy (adCRD) [25,26], while the latter has been associated with dominant CRD only [27,28]. No previously reported recessive RP loci are located in this critical interval, although *AIPL1* previously has been shown to cause LCA, autosomal dominant RP, and adCRD [26].

Given that genes associated with LCA (*RPE65*, *TULP1*, and *RDH12*) have also been implicated in retinitis pigmentosa [29-32], we sequenced the coding exons of *GUCY2D, PITPNM3,* and *AIPL1*, and identified only homozygous c.773G>C (p.R258P) missense and c.465G>T splice mutations in *AIPL1*. The clinical symptoms, age of onset, and the mode of inheritance in family 61032 are unambiguously consistent with autosomal recessive retinal degenerations, but given the clinical data available, it is difficult to distinguish LCA from arRP in these families. In family 61032, according to the history, the affected individuals developed their first recognized symptom, night blindness, after 3 years of age, although nystagmus, which frequently accompanies the early or congenital onset of blindness seen in LCA, occurred in individuals 8, 13, 15, and 19 but not in individuals 11, 12, and 14 in this family. In addition, according to the history and the medical records, the affected family members had good central vision during the first decade of life. This would be unusual for LCA, which is most often diagnosed in the first 6 months of life and characterized by the presence of nystagmus, poor visual acuity (VA), and a severely reduced or nondetectable electroretinogram at early stages [33-35]. Preservation of even the amounts of visual perception seen in the affected patients in this family at 16–29 years of age would be unusual in LCA. In addition, the clinical course of RP in these patients appeared to differ from that of classical AIPL1-related LCA in that the latter tend to have early and severe macular involvement [36-38]. Although the fundus photos from affected individuals show some macular changes (Figure 2), they are typical of those we have seen in other Pakistani families with arRP caused by various genes [14,15,39-41], and the clinical course including the initial symptom of night blindness and preservation of central vision through childhood is typical of relative preservation of macular function seen in RP rather than the early and severe macular involvement typical of LCA. Overall, this family certainly shows early onset retinal degeneration, lying in the clinical spectra of arRP and LCA. The retinal degeneration seen in family 61032 might correlate with the mutation in this family being a missense rather than nonsense or deletion and being predicted to be less severe by the various bioinformatic analyses. In contrast, the clinical history, signs, and symptoms of the affected individuals in family 61227 are more consistent with LCA, although once more it is difficult to place their phenotype definitively in either category.

AIPL1 encodes the aryl hydrocarbon receptor protein-like 1, found exclusively in rod photoreceptors in the human adult retina [42]. *Aipl1* knockout mice show normal development of the outer nuclear level, but early degeneration of rods and cones with disorganized and fragmented outer segments [43]. This appeared to occur through a reduction in rod cGMP phosphodiesterase (PDE6), a farnesylated protein regulating cGMP levels [43,44], although multiple phototransduction pathways appear to be affected [45]. In this regard, AIPL1

has been shown to bind NUB1 and inhibit NUB1-mediated degradation of FAT10 conjugated proteins [46]. Among other possible roles, *AIPL1* appears to act as a chaperone, aiding the proper assembly of newly synthesized PDE6 synthesis and thus affecting PDE6 turnover and cGMP regulation [47]. Therefore, the R258P mutation might have a specific effect on one or more functions of AIPL1, accounting for the differing phenotype seen in this family.

The R258P mutation lies toward the end of the second helix of the second TPR repeat unit in the TPR domain, although not actually a TPR motif or on a predicted binding surface (Figure 7A). TPR domains have been shown to be involved in several functions centering on protein–protein interactions and including chaperone, transcription, and protein transport activities. Substitution of a small uncharged proline residue for the larger positively charged arginine is not conservative, with a Blosum62 score of −2. The dihedral angles allowed by proline residues, which have stronger stereochemical constraints than any other amino acid residue, are not compatible with an alpha helical structure. Position 258 is predicted to lie just at the edge of an alpha helical region, which the R258P change disrupts and shortens. However, it is not predicted to cause significant disruption of the overall protein fold (Figure 7B), perhaps explaining why the phenotypic effects of this substitution are those of retinitis pigmentosa and not as severe as some cases of LCA. In contrast, although the p.H93_Q155 deletion seen in family 61227 does not directly involve either the FKBP_C or TPR domains, the loss of 63 amino acids between these two domains would be expected to affect the protein fold and distort their relative orientation.

Identification of two new recessive retinal degeneration loci in consanguineous Pakistani families emphasizes the genetic heterogeneity of this disorder. Further work on the functional aspects of this mutation promise to elucidate the multiple functions of AIPL1 in retinal photoreceptors, perhaps providing insights that will assist with eventual gene therapy [37]. Finally, identifying novel genes and mutations associated with autosomal recessive retinal degenerations will enhance our understanding of the disease at molecular level, leading to better treatments and therapeutics.

ACKNOWLEDGMENTS

The authors are thankful to all family members for their participation in this study. The authors are grateful to the staff of Layton Rehmatullah Benevolent Trust (LRBT) Hospital for clinical evaluation of affected individuals. This study was supported, in part by Higher Education Commission and Ministry of Science and Technology Islamabad, Pakistan and by NEI EY000272.

REFERENCES

1. Donders F. Beitrage zur pathologischen Anatomie des Auges. 2. Pigmentbildung in der Netzhaut. Arch Ophthalmol 1857; 3:139-65. .
2. Heckenlively JR, Yoser SL, Friedman LH, Oversier JJ. Clinical findings and common symptoms in retinitis pigmentosa. Am J Ophthalmol 1988; 105:504-11. [PMID: 3259404].
3. Bird AC. Retinal photoreceptor dystrophies LI. Edward Jackson Memorial Lecture. Am J Ophthalmol 1995; 119:543-62. [PMID: 7733180].
4. Bunker CH, Berson EL, Bromley WC, Hayes RP, Roderick TH. Prevalence of retinitis pigmentosa in Maine. Am J Ophthalmol 1984; 97:357-65. [PMID: 6702974].
5. Bundey S, Crews SJ. A study of retinitis pigmentosa in the city of Birmingham. J Med Genet 1986; 23:188-[PMID: 3712401].
6. Boughman JA, Conneally PM, Nance W. Population genetic studies of retinitis pigmentosa. Am J Hum Genet 1980; 32:223-5. [PMID: 7386458].
7. Boughman JA, Caldwell RJ. Genetic and clinical characterization of a survey population with retinitis pigmentosa. In: Daentl DL, editor. Clinical, Structural, and Biochemical Advances in Hereditary Eye Disorders. New York: Alan R. Liss Inc; 1982. p. 147–66.
8. Jay M. Figures and fantasies: the frequencies of the different genetic forms of retinitis pigmentosa. Birth Defects Orig Artic Ser 1982; 18:167-73. [PMID: 7171752].
9. Inglehearn CF. Molecular genetics of human retinal dystrophies. Eye (Lond) 1998; 12:Pt 3b571-9. [PMID: 9775219].
10. Koenig R. Bardet-Biedl syndrome and Usher syndrome. Dev Ophthalmol 2003; 37:126-40. [PMID: 12876834].
11. Standard for clinical electroretinography. International Standardization Committee. Arch Ophthalmol 1989; 107:816-9. [PMID: 2730397].
12. Naz S, Ali S, Riazuddin SA, Farooq T, Butt NH, Zafar AU, Khan SN, Husnain T, Macdonald IM, Sieving PA, Hejtmancik JF, Riazuddin S. Mutations in RLBP1 associated with fundus albipunctatus in consanguineous Pakistani families. Br J Ophthalmol 2011; 95:1019-24. [PMID: 21447491].
13. Riazuddin SA, Zulfiqar F, Zhang Q, Yao W, Li S, Jiao X, Shahzadi A, Amer M, Iqbal M, Hussnain T, Sieving PA, Riazuddin S, Hejtmancik JF. Mutations in the gene encoding the alpha-subunit of rod phosphodiesterase in consanguineous Pakistani families. Mol Vis 2006; 12:1283-91. [PMID: 17110911].
14. Naz S, Riazuddin SA, Li L, Shahid M, Kousar S, Sieving PA, Hejtmancik JF, Riazuddin S. A Novel Locus for Autosomal Recessive Retinitis Pigmentosa in a Consanguineous

Pakistani Family Maps to Chromosome 2p. Am J Ophthalmol 2010; 149:861-6. [PMID: 20227676].

15. Riazuddin SA, Zulfiqar F, Zhang Q, Sergeev YV, Qazi ZA, Husnain T, Caruso R, Riazuddin S, Sieving PA, Hejtmancik JF. Autosomal recessive retinitis pigmentosa is associated with mutations in RP1 in three consanguineous Pakistani families. Invest Ophthalmol Vis Sci 2005; 46:2264-70. [PMID: 15980210].
16. Grimberg J, Nawoschik S, Belluscio L, McKee R, Turck A, Eisenberg A. A simple and efficient non-organic procedure for the isolation of genomic DNA from blood. Nucleic Acids Res 1989; 17:8390-[PMID: 2813076].
17. Riazuddin SA, Yasmeen A, Zhang Q, Yao W, Sabar MF, Ahmed Z, Riazuddin S, Hejtmancik JF. A new locus for autosomal recessive nuclear cataract mapped to chromosome 19q13 in a Pakistani family. Invest Ophthalmol Vis Sci 2005; 46:623-6. [PMID: 15671291].
18. Lathrop GM, Lalouel JM. Easy calculations of lod scores and genetic risks on small computers. Am J Hum Genet 1984; 36:460-5. [PMID: 6585139].
19. Schäffer AA, Gupta SK, Shriram K, Cottingham RW. Avoiding recomputation in genetic linkage analysis. Hum Hered 1994; 44:225-37. [PMID: 8056435].
20. Reese MG, Eeckman FH, Kulp D, Haussler D. Improved splice site detection in Genie. J Comput Biol 1997; 4:311-23. [PMID: 9278062].
21. Hebsgaard SM, Korning PG, Tolstrup N, Engelbrecht J, Rouze P, Brunak S. Splice site prediction in Arabidopsis thaliana pre-mRNA by combining local and global sequence information. Nucleic Acids Res 1996; 24:3439-52. [PMID: 8811101].
22. Kumar P, Henikoff S, Ng PC. Predicting the effects of coding non-synonymous variants on protein function using the SIFT algorithm. Nat Protoc 2009; 4:1073-81. [PMID: 19561590].
23. Adzhubei IA, Schmidt S, Peshkin L, Ramensky VE, Gerasimova A, Bork P, Kondrashov AS, Sunyaev SR. A method and server for predicting damaging missense mutations. Nat Methods 2010; 7:248-9. [PMID: 20354512].
24. González-Pérez A, Lopez-Bigas N. Improving the assessment of the outcome of nonsynonymous SNVs with a consensus deleteriousness score, Condel. Am J Hum Genet 2011; 88:440-9. [PMID: 21457909].
25. Perrault I, Rozet JM, Calvas P, Gerber S, Camuzat A, Dollfus H, Chatelin S, Souied E, Ghazi I, Leowski C, Bonnemaison M, Le Paslier D, Frezal J, Dufier JL, Pittler S, Munnich A, Kaplan J. Retinal-specific guanylate cyclase gene mutations in Leber's congenital amaurosis. Nat Genet 1996; 14:461-4. [PMID: 8944027].
26. Sohocki MM, Bowne SJ, Sullivan LS, Blackshaw S, Cepko CL, Payne AM, Bhattacharya SS, Khaliq S, Qasim Mehdi S, Birch DG, Harrison WR, Elder FF, Heckenlively JR, Daiger SP. Mutations in a new photoreceptor-pineal gene on 17p cause Leber congenital amaurosis. Nat Genet 2000; 24:79-83. [PMID: 10615133].
27. Balciuniene J, Johansson K, Sandgren O, Wachtmeister L, Holmgren G, Forsman K. A gene for autosomal dominant progressive cone dystrophy (CORD5) maps to chromosome 17p12-p13. Genomics 1995; 30:281-6. [PMID: 8586428].
28. Köhn L, Kadzhaev K, Burstedt MS, Haraldsson S, Hallberg B, Sandgren O, Golovleva I. Mutation in the PYK2-binding domain of PITPNM3 causes autosomal dominant cone dystrophy (CORD5) in two Swedish families. Eur J Hum Genet 2007; 15:664-71. [PMID: 17377520].
29. Morimura H, Fishman GA, Grover SA, Fulton AB, Berson EL, Dryja TP. Mutations in the RPE65 gene in patients with autosomal recessive retinitis pigmentosa or leber congenital amaurosis. Proc Natl Acad Sci USA 1998; 95:3088-93. [PMID: 9501220].
30. Marlhens F, Bareil C, Griffoin JM, Zrenner E, Amalric P, Eliaou C, Liu SY, Harris E, Redmond TM, Arnaud B, Claustres M, Hamel CP. Mutations in RPE65 cause Leber's congenital amaurosis. Nat Genet 1997; 17:139-41. [PMID: 9326927].
31. Banerjee P, Kleyn PW, Knowles JA, Lewis CA, Ross BM, Parano E, Kovats SG, Lee JJ, Penchaszadeh GK, Ott J, Jacobson SG, Gilliam TC. TULP1 mutation in two extended Dominican kindreds with autosomal recessive retinitis pigmentosa. Nat Genet 1998; 18:177-9. [PMID: 9462751].
32. Perrault I, Hanein S, Gerber S, Barbet F, Ducroq D, Dollfus H, Hamel C, Dufier JL, Munnich A, Kaplan J, Rozet JM. Retinal dehydrogenase 12 (RDH12) mutations in leber congenital amaurosis. Am J Hum Genet 2004; 75:639-46. [PMID: 15322982].
33. Lambert SR, Kriss A, Taylor D, Coffey R, Pembrey M. Follow-up and diagnostic reappraisal of 75 patients with Leber's congenital amaurosis. Am J Ophthalmol 1989; 107:624-31. [PMID: 2658617].
34. Koenekoop RK. An overview of Leber congenital amaurosis: a model to understand human retinal development. Surv Ophthalmol 2004; 49:379-98. [PMID: 15231395].
35. Traboulsi EI, Koenekoop R, Stone EM. Lumpers or splitters? The role of molecular diagnosis in Leber congenital amaurosis. Ophthalmic Genet 2006; 27:113-5. [PMID: 17148037].
36. Pennesi ME, Stover NB, Stone EM, Chiang PW, Weleber RG. Residual electroretinograms in young Leber congenital amaurosis patients with mutations of AIPL1. Invest Ophthalmol Vis Sci 2011; 52:8166-73. [PMID: 21900377].
37. Testa F, Surace EM, Rossi S, Marrocco E, Gargiulo A, Di Iorio V, Ziviello C, Nesti A, Fecarotta S, Bacci ML, Giunti M, Della Corte M, Banfi S, Auricchio A, Simonelli F. Evaluation of Italian patients with leber congenital amaurosis due to AIPL1 mutations highlights the potential applicability of gene therapy. Invest Ophthalmol Vis Sci 2011; 52:5618-24. [PMID: 21474771].
38. Jacobson SG, Cideciyan AV, Aleman TS, Sumaroka A, Roman AJ, Swider M, Schwartz SB, Banin E, Stone EM. Human retinal disease from AIPL1 gene mutations: foveal cone loss with minimal macular photoreceptors and rod function

remaining. Invest Ophthalmol Vis Sci 2011; 52:70-9. [PMID: 20702822].

39. Ali S, Riazuddin SA, Shahzadi A, Nasir IA, Khan SN, Husnain T, Akram J, Sieving PA, Hejtmancik JF, Riazuddin S. Mutations in the beta-subunit of rod phosphodiesterase identified in consanguineous Pakistani families with autosomal recessive retinitis pigmentosa. Mol Vis 2011; 17:1373-80. [PMID: 21655355].

40. Zhang Q, Zulfiqar F, Xiao X, Riazuddin SA, Ahmad Z, Caruso R, MacDonald I, Sieving P, Riazuddin S, Hejtmancik JF. Severe retinitis pigmentosa mapped to 4p15 and associated with a novel mutation in the PROM1 gene. Hum Genet 2007; [PMID: 17605048].

41. Zhang Q, Zulfiqar F, Xiao X, Riazuddin SA, Ayyagari R, Sabar MF, Caruso R, Sieving P, Riazuddin S, Hejtmancik JF. Severe autosomal recessive retinitis pigmentosa maps to chromosome 1p13.3-p21.2 between D1S2896 and D1S457 but outside ABCA4. Hum Genet 2005; 118:356-65. [PMID: 16189710].

42. van der Spuy J, Chapple JP, Clark BJ, Luthert PJ, Sethi CS, Cheetham ME. The Leber congenital amaurosis gene product AIPL1 is localized exclusively in rod photoreceptors of the adult human retina. Hum Mol Genet 2002; 11:823-31. [PMID: 11929855].

43. Ramamurthy V, Niemi GA, Reh TA, Hurley JB. Leber congenital amaurosis linked to AIPL1: a mouse model reveals destabilization of cGMP phosphodiesterase. Proc Natl Acad Sci USA 2004; 101:13897-902. [PMID: 15365178].

44. Liu X, Bulgakov OV, Wen XH, Woodruff ML, Pawlyk B, Yang J, Fain GL, Sandberg MA, Makino CL, Li T. AIPL1, the protein that is defective in Leber congenital amaurosis, is essential for the biosynthesis of retinal rod cGMP phosphodiesterase. Proc Natl Acad Sci USA 2004; 101:13903-8. [PMID: 15365173].

45. Makino CL, Wen XH, Michaud N, Peshenko IV, Pawlyk B, Brush RS, Soloviev M, Liu X, Woodruff ML, Calvert PD, Savchenko AB, Anderson RE, Fain GL, Li T, Sandberg MA, Dizhoor AM. Effects of low AIPL1 expression on phototransduction in rods. Invest Ophthalmol Vis Sci 2006; 47:2185-94. [PMID: 16639031].

46. Bett JS, Kanuga N, Richet E, Schmidtke G, Groettrup M, Cheetham ME, van der Spuy J. The inherited blindness protein AIPL1 regulates the ubiquitin-like FAT10 pathway. PLoS ONE 2012; 7:e30866-[PMID: 22347407].

47. Kolandaivelu S, Huang J, Hurley JB, Ramamurthy V. AIPL1, a protein associated with childhood blindness, interacts with alpha-subunit of rod phosphodiesterase (PDE6) and is essential for its proper assembly. J Biol Chem 2009; 284:30853-61. [PMID: 19758987].

Articles are provided courtesy of Emory University and the Zhongshan Ophthalmic Center, Sun Yat-sen University, P.R. China. The print version of this article was created on 6 January 2014. This reflects all typographical corrections and errata to the article through that date. Details of any changes may be found in the online version of the article.